Manuscript prepared for Atmos. Chem. Phys.
with version 2014/07/29 7.12 Copernicus papers of the LaTeX class copernicus.cls.
Date: 22 October 2014

Comparing turbulent parameters obtained from LITOS and radiosonde measurements

A. Schneider, M. Gerding, and F.-J. Lübken

Leibniz-Institute of Atmospheric Physics at the University of Rostock, Kühlungsborn, Germany

Correspondence to: A. Schneider (schneider@iap-kborn.de)

Abstract. Stratospheric turbulence is important for the mixing of trace species and the energy balance, but direct measurements are sparse due to the required resolution and accuracy. Recently, turbulence parameters such as the energy dissipation rate ε were inferred from standard radiosonde data by means of a Thorpe analysis. To this end, layers with vertically decreasing potential temperature are analysed, which is expected to indicate turbulence. Such an application assumes a proportionality between the Thorpe length L_T and the Ozmidov scale L_O. While this relation is accepted for the ocean, experimental evidence for such proportionality in the stratosphere is sparse. We have developed a high-resolution (8 kHz) turbulence measurement system called LITOS, which for the first time resolves the inner scale of turbulence in the stratosphere. Therewith the energy dissipation rate ε can be determined by spectral analysis. This independent value for ε enables us to check the relation $L_O \propto L_T$. It turns out that no proportionality can be seen in our measurements. Furthermore, dissipation rates obtained from radiosondes deviate up to a factor of ~ 3000 to those obtained by spectral analysis. Some turbulent layers measured by LITOS are not observed by the radiosonde at all, and vice versa.

1 Introduction

Although the stratosphere is mostly stably stratified, breaking of gravity waves and instabilities cause turbulence and energy dissipation. This modifies the energy transport from the troposphere to the mesosphere. The amount of energy converted into heat is described by the turbulent energy dissipation rate ε. Moreover, turbulence is an important parameter for the vertical mixing of trace species. As in the stratosphere turbulent dissipation occurs on small scales of centimetres and below, measurements are technically challenging and therefore sparse (e. g., Barat, 1982; Theuerkauf et al., 2011).

In order to enlarge the amount of turbulence measurements without complicated technical development, it has been proposed to extract turbulence parameters such as ε from standard radiosonde data (vertical resolution 5 m), as radiosoundings are performed daily from a worldwide net of stations (Clayson and Kantha, 2008). The evaluation uses the method developed by Thorpe (1977, 2005) to detect static instabilities as a proxy for turbulence. Note that such a measurement is somewhat different from measuring the turbulent motions directly, as done by LITOS. For example, within an instability turbulence may have not yet been developed, or on the other hand, turbulence might be still active while the instability has already deceased. Additionally, turbulence may not be related to static instabilities at all.

The Thorpe analysis of unstable layers is done by comparing a measured potential temperature profile to an equivalent (statically) stable one obtained by sorting. This means that the order of the data points is changed upwards and downwards to yield a statically stable profile with monotonously increasing potential temperature. Precisely, the Thorpe displacement D_T is defined by the vertical displacements needed for the sorting, i. e. if an air parcel at altitude z_j is sorted to z_k, then the Thorpe displacement at z_j is $D_T(z_j) = z_j - z_k$. The Thorpe length is the root mean square of the Thorpe displacements taken over an unstable layer,

$$L_T := \mathrm{rms}(D_T). \tag{1}$$

It describes the distance on which heavier air parcels are carried above lighter ones. Wilson et al. (2011, 2010) use the Thorpe method for statistical analysis without computing dissipation rates.

The Ozmidov length scale

$$L_O := \alpha \sqrt{\frac{\varepsilon}{N^3}}, \tag{2}$$

where ε is the (kinetic) energy dissipation rate, N the Brunt–Väisälä frequency and α a numerical constant near unity, represents the vertical scales of the largest turbulent eddies (Ozmidov, 1965). For the determination of the dissipation rate from a Thorpe analysis, the key assumption is a proportionality between Thorpe and Ozmidov lengths, $L_O \propto L_T$. This relation has been extensively studied in the ocean, and the assumption is fulfilled to a good extent (Thorpe, 2005; Dillon, 1982; Wesson and Gregg, 1994). But for the atmosphere there are only few examinations of the proportionality (e. g. Gavrilov et al., 2005; Kantha and Hocking, 2011; Wilson et al., 2014). With our new high-resolved instrument LITOS (Leibniz-Institute Turbulence Observations in the Stratosphere) (Theuerkauf et al., 2011), the energy dissipation rate ε is obtained independent of L_T by means of spectral analysis of wind fluctuations. Thus it is possible to check the relation $L_O \propto L_T$.

Please note that our comparison involves two parameters: (a) evaluation method (Thorpe or spectral analysis) and (b) vertical resolution (low or high). We concentrate on results from high-resolved spectral analysis (as very precise method of ε determination) and low-resolved Thorpe analysis. Such a Thorpe evaluation of radiosonde data has been proposed for extensive use (Clayson and Kantha, 2008; Love and Geller, 2012). Note that Love and Geller (2012) call 1 Hz (5 m) high resolution, while we call it low resolution (compared to LITOS with 8 kHz). In principle, the Thorpe analysis can also be performed on data with higher resolution, as done, e. g., by Luce et al. (2002) for temperature data with 50 Hz sampling rate; however, these data are rarely available compared to standard radiosonde. Besides, a kind of spectral analysis can be used to determine dissipation rates from low-resolution wind data (Barat, 1982), but this method depends on the absolute value of the wind velocity which is not available for our measurements (see next section).

In Sect. 2, the measurement principle of LITOS and the determination of the energy dissipation rates with both methods are shortly reviewed. The independent measurements of L_O and L_T are compared in Sect. 3. Section 4 shows results for the energy dissipation rate ε from both a Thorpe analysis and our high-resolved spectral analysis. Conclusions are drawn in Sect. 5.

2 Instrumentation and methods

As described in Theuerkauf et al. (2011), LITOS is a balloon-borne instrument which measures winds with high vertical resolution of millimetres. The wind sensor is a constant temperature anemometer (CTA), which facilitates the cooling effect on a heated wire of 5 µm diameter. To infer wind velocities from the anemometer voltage, a calibration in the same ambient conditions (pressure, temperature) is required. This is not possible for a balloon flight, as the pressure varies within several orders of magnitude during the flight. Nevertheless, we are only interested in the spectral form, and the absolute values are not important (see below); therefore we use the anemometer voltage for the analysis. The vertical resolution is obtained by applying a sample rate of 8 kHz with a balloon ascent rate of $5\,\mathrm{m\,s^{-1}}$. Up to date, three flights on large ($\sim 10\,000\,\mathrm{m^3}$) balloons were performed, namely BEXUS 6, 8 and 12 in 2008, 2009 and 2011, respectively. They were launched at Kiruna (68° N, 21° E) in autumn. For BEXUS 6, the radiosonde data are partly disturbed so that it is not considered in this article.

The left panel in Fig. 1 shows an example of a time series of the anemometer voltage of the BEXUS 12 flight. Large-scale motions have already been removed by subtracting a spline. At altitudes with small variations ($\lesssim 1$ mV, e. g., from 10.28 to 10.3 km), the signal mainly shows instrumental noise; this corresponds to a calm region. Large fluctuations, as in the height range of 10.18 to 10.28 km, correspond to turbulence. Note that there is a sub-structure which divides the turbulent region into different patches. For the patch from 10.27 to 10.28 km (shaded in the graph), the power spectral density (PSD) is plotted in the right panel of Fig. 1 (blue curve). An inertial regime with a $-5/3$ slope and the transition to the viscous subrange with a -7 slope is identified. The part below $\sim 10^{-2}$ m spatial scale with approximately constant PSD corresponds to the instrumental noise level. As the transition to the inertial range is resolved, a fit of the Heisenberg (1948) model in the form given by Lübken (1992) is applied to the experimental data (red curve). This gives the inner scale l_0, i. e. the transition from the inertial to the viscous subrange. In the example, $l_0 = 1.9 \times 10^{-2}\,\mathrm{m} \pm 4.5 \times 10^{-3}\,\mathrm{m}$ (fit error). Note that l_0 does not depend on the absolute value of the PSD, only on identifying the bend in the spectrum. From the inner scale, the energy dissipation rate is obtained by

$$\varepsilon = c^4 \frac{\nu^3}{l_0^4}, \tag{3}$$

where ν is the kinematic viscosity (derived from the radiosonde measurement of temperature and pressure on the same gondola), and $c = 5.7$ (Theuerkauf et al., 2011; Haack et al., 2014). For the example in Fig. 1, $\varepsilon = 3.2 \times 10^{-4}\,\mathrm{W\,kg^{-1}} \pm 3.0 \times 10^{-4}\,\mathrm{W\,kg^{-1}}$.

In order to obtain a vertical profile of energy dissipation rate, a sliding window of 5 s (roughly 25 m altitude) is used. For each window, ε is computed according to the procedure described above. For non-turbulent spectra, ε is set to zero. A spectrum is regarded as non-turbulent if the noise-level detection fails, if the inner scale l_0 is not within the fit range, if ε has implausible values (less than zero or greater than $100\,\mathrm{W/kg}$), or if the mean distance between the fit and the data is larger than a fixed threshold. That means the decision is made automatically based on a set of objective criteria. The resulting ε profile has a vertical resolution of ~ 10 m due to the selected overlap.

The Thorpe analysis is performed according to the procedure described in Wilson et al. (2011) on data from a Vaisala RS92 radiosonde, which was on the same gondola as the CTA sensors. Moisture is cared for using the routine given by Wilson et al. (2013). To this end, saturated regions are detected, and a composite potential temperature profile Θ_* is computed by integration of $\partial\Theta/\partial z$ using the moist buoyancy frequency within those saturated regions and the dry buoyancy frequency otherwise. The left panel of Fig. 2 shows the potential temperature profile for the BEXUS 12 flight. In the inset, the part from 15.35 to 15.80 km is magnified for better visibility of instabilities, which manifest as negative gradients of potential temperature. The Thorpe displacement is shown in the right panel of Fig. 2. Large displacements correspond to large vertical extents of unstable layers. To identify unstable layers and their vertical extension, the cumulative sum of the Thorpe displacement (which is negative within an unstable region and zero within a stable one) is used. To select real overturns and discard negative potential temperature gradients originating from measurement noise, a statistical test is applied. To this end, the range of the potential temperatures within an inversion is compared with the range of a pure noise sample of the same length with standard deviation of the measurement noise (Wilson et al., 2010). For each detected unstable layer, the Thorpe length is computed according to Eq. (1). Only significant overturns with a 99 % percentile are used, discarding ~ 45 % (BEXUS 8) and ~ 30 % (BEXUS 12), respectively, of the inversions as noise-induced. The mean trend-to-noise ratio (TNR) is $\bar{\xi} = 1.7$ for the BEXUS 8 flight and $\bar{\xi} = 4.1$ for the BEXUS 12 flight.

Several thin layers of only 10 m or 20 m passed the significance test. We are aware that this is on the edge of radiosonde capability. Nevertheless, LITOS also shows many thin layers. Ignoring the thin layers, e. g., by smoothing the Θ_* profile prior to Thorpe sorting would result in much less coincident layers especially in the stratosphere and, by this, bias the comparison. In order to avoid any a-priori biases we take the significant thin layers in the radiosonde data into account.

3 Comparison of Thorpe and Ozmidov scales

A plot of the Thorpe length for the BEXUS 12 flight is shown in the left panel of Fig. 3. Unstable layers take up 50 % of the altitude and can be found in the whole range. Large Thorpe lengths stand out, e. g., at 5 km, between 5 and 10 km and near 25 km altitude, corresponding to the large values of D_T in the right panel of Fig. 2. Mean values of L_T are 29 m in the troposphere and 22 m in the stratosphere, i. e. the Thorpe length is slightly larger in the less stable troposphere.

The Ozmidov scale is computed from the energy dissipation rate obtained by LITOS, using Eq. (2) and $\alpha = 1$. The Brunt–Väisälä frequency N is calculated from the radiosonde data as it only slowly varies with altitude. In that computation, the sorted potential temperature profile is used instead of the original data, because a background stratification is needed and an imaginary N shall be avoided (Dillon, 1982, Sect. 3). The result for the BEXUS 12 flight is plotted in the right panel of Fig. 3 (cyan curve). According to LITOS, 53 % of the atmosphere is turbulent, i. e. $\varepsilon > 0$ and hence $L_\mathrm{O} > 0$.

Figure 4 shows the Thorpe length and the Ozmidov scale for the altitude range of 15.35 km to 15.80 km. As LITOS computes ε on a constant grid independent of the layers, the substructure of larger turbulent layers can be seen (e. g., from $\sim$ 15.5 km to 15.62 km), while the Thorpe length is a per-layer value by construction. Some layers are only detected by either LITOS or the radiosonde. For example, from 15.410 km to 15.443 km and from 15.706 km to 15.789 km LITOS observes turbulence while the Thorpe method does not. At the first mentioned altitude region, the potential temperature gradient is positive , so that the Thorpe method is blind for the turbulent motions. At the second one, the decrease of potential temperature is not significant. On the other hand, from 15.384 km to 15.401 km and from 15.455 km to 15.475 km, the Thorpe analysis observes instability while no turbulent motions can be detected by LITOS. Potentially, turbulence has not yet been developed by the static instability detected by the Thorpe method. A final answer cannot be given from our data. The slightly different altitudes of layers observed by both systems might be due to quantisation effects.

In order to do a comparison between both length scales, the layers where both methods detect turbulence are selected. For BEXUS 8 (BEXUS 12), 86 % (69 %) of the significant unstable layers are also detected by LITOS, and 90 % (88 %) of the layers detected by LITOS intersect with a significant unstable layer. The energy dissipation rate (obtained from LITOS) is averaged over the layer (as detected by the Thorpe analysis of radiosonde data). Such means over a Thorpe layer will be denoted by averaging brackets $\langle\cdot\rangle$. For each unstable layer, the resulting $\langle\varepsilon\rangle$ is plugged into Eq. (2) to infer an Ozmidov scale $\overline{L_\mathrm{O}} = \sqrt{\langle\varepsilon\rangle/\langle N\rangle^3}$ for the layer. The blue curve in the right panel of Fig. 3 shows a plot for the BEXUS 12 flight. The layer near 5 km with large L_T, e. g., is also seen in $\overline{L_\mathrm{O}}$, but less pronounced. In contrast, at $\sim$10 km altitude the Ozmidov scale is larger than the Thorpe scale. Mean values of $\overline{L_\mathrm{O}}$ are 15 m in the troposphere and 6 m (i. e. only half the value) in the stratosphere. Thus, in qualitative agreement with Eq. (2), the less stable troposphere shows on average a larger Ozmidov scale, i. e. larger eddies. As the Thorpe length shows a similar behaviour (see above), this generally supports the assumption of a relation between L_T and L_O.

In Fig. 5 Ozmidov scale $\overline{L_\mathrm{O}}$ and Thorpe length L_T are plotted against each other for those 136 (175) significant unstable layers of the BEXUS 8 (BEXUS 12) flight where turbulence has been detected by LITOS. Both length scales are in the same order of magnitude, but no direct relation between

them can be seen in either flight. The correlation coefficient between both is 0.32 for BEXUS 8 and 0.33 for BEXUS 12. Note that L_T is limited by the resolution of the radiosonde (~ 10 m).

The histograms at the top and right axes in Fig. 5 show the distributions for $\overline{L_O}$ and L_T, respectively, for the composite dataset of BEXUS 8 and BEXUS 12. The maximum for the Thorpe length is slightly larger than for the Ozmidov scale. The decrease towards large scales is similar for both lengths. At small scales L_T is limited by the resolution of the radiosonde which produces the cut-off at 10 m, while the histogram for $\overline{L_O}$ shows a continuous decrease.

In contrast to our measurements, an approximate proportionality between Thorpe and Ozmidov lengths is observed in the ocean (e. g., Dillon, 1982; Wesson and Gregg, 1994; Thorpe, 2005). For example, Wesson and Gregg (1994) find that most of their data fall between $L_O = 4L_T$ and $L_O = (1/4)L_T$ with a range from 10^{-2} m to 10^2 m. This is the basis for applying the Thorpe analysis on atmospheric data. Several authors (e. g., Gavrilov et al., 2005; Clayson and Kantha, 2008; Kantha and Hocking, 2011) inferred energy dissipation rates from the Thorpe analysis by plugging $L_O = c\,L_T$ into Eq. (2) and solving for ε, thus getting

$$\varepsilon = c^2 L_T^2 N^3. \tag{4}$$

Knowledge about the constant c^2 is very limited (see discussion below), and only Gavrilov et al. (2005) provide some information based on stratospheric data. With our high-resolved wind data we can determine this constant independently. Wijesekera et al. (1993) found the distribution of the ratio L_T/L_O to be lognormal, which implies $(L_O/L_T)^2 = c^2$ to be lognormal as well. Logarithmic histograms of $(\overline{L_O}/L_T)^2$ for the BEXUS 8 and BEXUS 12 flights are presented in Fig. 6. The red curves display the most likely normal distributions for the logarithmic data. They show a sufficient agreement to the histograms and are both centred around ~ 0.1. The distribution of values is fairly broad: the full width half maximum (FWHM) spans ~ 1.9 orders of magnitude.

4 Energy dissipation rates

The relation between the energy dissipation rate ε and the length scales discussed above involves the Brunt–Väisälä frequency, see Eqs. (2) and (4). Thus the ε values computed from LITOS via spectral analysis and the ones from the radiosonde via Thorpe analysis have to be compared separately.

The left panel of Fig. 7 shows an altitude profile of energy dissipation rates obtained from the Thorpe analysis of the radiosonde on BEXUS 12, assuming $L_O = c\,L_T$ with $c^2 = 0.3$ as in Clayson and Kantha (2008). In the right panel, the altitude profile of energy dissipation obtained from LITOS is plotted in cyan, while the blue curve depicts the mean $\langle\varepsilon\rangle$ over the unstable layers detected by the Thorpe analysis, for comparability. On average, the values are in the same order of magnitude, and the profiles have a similar structure. The large dissipation near ~ 10 km in the CTA data does not stand out in the Thorpe analysis. The mean value over all significant unstable layers from Thorpe, 1 mW kg^{-1}, is larger than the one from LITOS, 0.3 mW kg^{-1}. For BEXUS 8 the averages are 3 mW kg^{-1} from Thorpe and 2 mW kg^{-1} from LITOS. That fits to the fact that the used value for c^2, 0.3, is larger than the one obtained from our own data, $c^2 = 0.1$ (cf. Fig. 6). If the whole ε profile (not only the unstable layers detected by Thorpe) is taken into account, the average dissipation rate obtained by LITOS is 0.4 mW kg^{-1} for BEXUS 12 and 2 mW kg^{-1} for BEXUS 8. To get a closer look, the deviation of $\langle\varepsilon\rangle$ from LITOS to ε inferred from the Thorpe analysis indicated by the ratio $\langle\varepsilon_{\mathrm{LITOS}}\rangle/\varepsilon_{\mathrm{Thorpe}}$ of the blue and green curves in Fig. 7 is plotted in Fig. 8. It reveals a large range of 5 orders of magnitude. Overall, for 71 % (BEXUS 8: 64 %) of the layers, ε inferred from the Thorpe analysis is larger than the value from the spectral analysis. That the ratio is sometimes larger and sometimes smaller than unity illustrates that the most likely value of c^2 does not contain the whole information, but the width of the distribution is important. The correlation coefficient between $\langle\varepsilon_{\mathrm{LITOS}}\rangle$ and $\varepsilon_{\mathrm{Thorpe}}$ is 0.06 (BEXUS 8: 0.39). Due to the influence of the Brunt–Väisälä frequency, pronounced peaks in L_O or L_T (Fig. 3) do not necessarily correspond to large ε (Fig. 7), e. g., at ~ 5 km.

5 Discussion and conclusions

In this paper, the first extensive examination of the relation between the Thorpe length L_T and Ozmidov scale L_O for stratospheric conditions was performed, using the new high-resolution instrument LITOS and a radiosonde on the same gondola. Therewith, the assumption for computing energy dissipation rates ε from a Thorpe analysis of standard radiosondes, namely the proportionality $L_O \propto L_T$, was checked. In our data no obvious relation between $\overline{L_O}$ and L_T can be seen, particularly no proportionality. The proportionality "constant" used in radiosonde analyses, $c^2 = (\overline{L_O}/L_T)^2$, shows a very broad distribution with a width of ~ 2 orders of magnitude. This is also reflected in the large deviation of ε values up to a factor of ~ 3000 obtained with both methods. Nevertheless, although the values for individual layers are highly variable, the mean of c^2 is 0.1 for both BEXUS 12 and BEXUS 8, which is close to 0.3 used by Clayson and Kantha (2008), who reviewed oceanic measurements to obtain that value. Kantha and Hocking (2011) obtained $c^2 = 1.0$ by a comparison of radiosonde data to radar measurements. Gavrilov et al. (2005) used $c^2 = 1.32$ ($c = 1.15$) referring to a French thesis; this value was obtained from selected thick stratospheric layers (> 200 m) with statistically homogeneous turbulence. However, in those publications no data basis, distribution width or error is given. Recently, Wilson et al. (2014) reported a few case studies of turbulent layers

in the troposphere detected simultaneously by radar and balloon; using their reported estimates of L_T and L_O leads to values of c^2 between 0.1 and 1.6.

One reason for discrepancies from the proportionality $L_O \propto L_T$ may be that large overturns might change significantly during the time the sensor needs to fly through the layer, so that the sorting procedure makes no sense anymore. Furthermore, direct numerical simulations by Smyth and Moum (2000) indicate that L_O/L_T is not constant, but depends on the age of turbulence.

Some turbulent layers are not detected at all by the Thorpe analysis. Those are not associated with a (significant) negative gradient of potential temperature, which is necessary for detection by the Thorpe method. Not all turbulence is related to static instabilities. Even if initially a negative potential temperature gradient may have occurred, it is removed by the turbulent motions which outlive the instability; such fossil turbulence cannot be detected by the Thorpe method. Apart from that, turbulent layers may be too thin to be observed with the relatively coarse vertical resolution of the radiosonde. On the other hand, some unstable layers detected by the Thorpe analysis are not observed by LITOS. An explanation is that the static instability may not yet have lead to turbulent motions. In these cases, a correspondence between both measurements is not expected.

Not all layers are detected by both systems. Of the significant layers detected by the Thorpe analysis, 86 % (BEXUS 8) and 69 % (BEXUS 12) are also detected by LITOS. For BEXUS 12, the mean thickness of significant unstable layers as detected by the Thorpe analysis is 53 m. The mean thickness of those significant layers also detected by LITOS is 63 m, that of significant layers not detected by LITOS only 31 m. That means that the simultaneous detection depends on the size of the layer; mainly thin layers are detected by only one method. But as this only applies to $\lesssim 30$ % of the layers, and those layers were taken out of the comparison, the bias for our results should be small.

For LITOS, the detection limit for l_0 on small scales (i. e. high frequencies or large ε) is given by the sampling rate. This limit has been encountered in a few cases for small regions where the inertial range extends further than the Nyquist limit of 4 kHz. For large scales (i. e. low frequencies or small ε), the detection limit is determined by the trend removal and the window length. As a reasonable part of the inertial range has to be resolved to enable a fit, the limit is estimated to ~ 1 m. The maximal identified l_0 values of 10 cm and 8.7 cm for BEXUS 8 and BEXUS 12, respectively, were far below this limit. That means that these limitations do not affect the results.

Up to date, we have only two flights with data usable for the analysis presented in this paper, namely BEXUS 8 and BEXUS 12, which both took place at polar latitudes near autumn equinox. Of course they cannot represent the whole variability of the stratosphere. Nevertheless, although there are differences between both flights, such as dissipation rates being on average one order of magnitude higher for BEXUS 8, these are not relevant for the results discussed above. More flights with our new high-resolution instrument are planned to broaden the data basis.

Our results question the applicability of the Thorpe analysis for the extraction of energy dissipation rates for individual turbulent layers. Nevertheless, statements in the statistical mean seem to be possible. Further research on the relation between Thorpe and Ozmidov lengths and the temporal evolution of turbulence is necessary.

Acknowledgements. The data from the BEXUS 8 flight were kindly provided by Anne Haack. The BEXUS programme was financed by the German Aerospace Center (DLR) and the Swedish National Space Board (SNSB). We are grateful for the support by the "International Leibniz Graduate School for Gravity Waves and Turbulence in the Atmosphere and Ocean" (ILWAO) funded by the Leibniz Association (WGL). Furthermore, we would like to thank Lars Umlauf for helpful discussions.

References

Barat, J.: Some characteristics of clear-air turbulence in the middle stratosphere, J. Atmos. Sci., 39, 2553–2564, doi:10.1175/1520-0469(1982)039<2553:SCOCAT>2.0.CO;2, 1982.

Clayson, C. A. and Kantha, L.: On turbulence and mixing in the free atmosphere inferred from high-resolution soundings, J. Atmos. Ocean. Tech., 25, 833–852, doi:10.1175/2007JTECHA992.1, 2008.

Dillon, T. M.: Vertical overturns: A comparison of Thorpe and Ozmidov length scales, J. Geophys. Res., 87, 9601–9613, 1982.

Gavrilov, N. M., Luce, H., Crochet, M., Dalaudier, F., and Fukao, S.: Turbulence parameter estimations from high-resolution balloon temperature measurements of the MUTSI-2000 campaign, Ann. Geophys., 23, 2401–2413, doi:10.5194/angeo-23-2401-2005, 2005.

Haack, A., Gerding, M., and Lübken, F.-J.: Characteristics of stratospheric turbulent layers measured by LITOS and their relation to the Richardson number, J. Geophys. Res., 119, 10 605–10 618, doi:10.1002/2013JD021008, 2014.

Heisenberg, W.: Zur statistischen Theorie der Turbulenz, Z. Phys., 124, 628–657, doi:10.1007/BF01668899, 1948.

Kantha, L. and Hocking, W.: Dissipation rates of turbulence kinetic energy in the free atmosphere: MST radar and radiosondes, J. Atmos Sol.-Terr. Phy., 73, 1043–1051, doi:10.1016/j.jastp.2010.11.024, 2011.

Love, P. T. and Geller, M. A.: Research using high (and higher) resolution radiosonde data, T. Am. Geophys. Un., 93, 337–338, doi:10.1029/2012EO350001, 2012.

Lübken, F.-J.: On the extraction of turbulent parameters from atmospheric density fluctuations, J. Geophys. Res., 97, 20 385–20 395, doi:10.1029/92JD01916, 1992.

Luce, H., Fukao, S., Dalaudier, F., and Crochet, M.: Strong Mixing Events Observed near the Tropopause with the MU Radar and High-Resolution Balloon Techniques, J. Atmos. Sci., 59, 2885–2896, doi:10.1175/1520-0469(2002)059<2885:SMEONT>2.0.CO;2, 2002.

Ozmidov, R. V.: On the turbulent exchange in a stably stratified ocean, Izv. AN. Fiz. Atmos. Ok., 1, 853–860, translated from Russian by Danielle and Victor Barcilon, 1965.

Smyth, W. D. and Moum, J. N.: Length scales of turbulence in stably stratified mixing layers, Phys. Fluids, 12, 1327–1342, doi:10.1063/1.870385, 2000.

Theuerkauf, A., Gerding, M., and Lübken, F.-J.: LITOS – a new balloon-borne instrument for fine-scale turbulence soundings in the stratosphere, Atmos. Meas. Tech., 4, 55–66, doi:10.5194/amt-4-55-2011, 2011.

Thorpe, S. A.: Turbulence and mixing in a Scottish loch, Philos. Tr. R. Soc. S-A, 286, 125–181, doi:10.1098/rsta.1977.0112, 1977.

Thorpe, S. A.: The Turbulent Ocean, Cambridge University Press, Cambridge, section 6.3.2, 2005.

Wesson, J. C. and Gregg, M. C.: Mixing at Camarinal Sill in the Strait of Gibraltar, J. Geophys. Res., 99, 9847–9878, doi:10.1029/94JC00256, 1994.

Wijesekera, H. W., Dillon, T. M., and Padman, L.: Some statistical and dynamical properties of turbulence in the oceanic pycnocline, J. Geophys. Res., 98, 22 665–22 679, doi:10.1029/93JC02352, 1993.

Wilson, R., Luce, H., Dalaudier, F., and Lefrère, J.: Turbulence patch identification in potential density or temperature profiles, J. Atmos. Ocean. Tech., 27, 977–993, doi:10.1175/2010JTECHA1357.1, 2010.

Wilson, R., Dalaudier, F., and Luce, H.: Can one detect small-scale turbulence from standard meteorological radiosondes?, Atmos. Meas. Tech., 4, 795–804, doi:10.5194/amt-4-795-2011, 2011.

Wilson, R., Luce, H., Hashiguchi, H., Shiotani, M., and Dalaudier, F.: On the effect of moisture on the detection of tropospheric turbulence from in situ measurements, Atmos. Meas. Tech., 6, 697–702, doi:10.5194/amt-6-697-2013, 2013.

Wilson, R., Luce, H., Hashiguchi, H., Nishi, N., and Yabuki, Y.: Energetics of persistent turbulent layers underneath mid-level clouds estimated from concurrent radar and radiosonde data, J. Atmos. Sol.-Terr. Phy., 118, Part A, 78–89, doi:10.1016/j.jastp.2014.01.005, 2014.

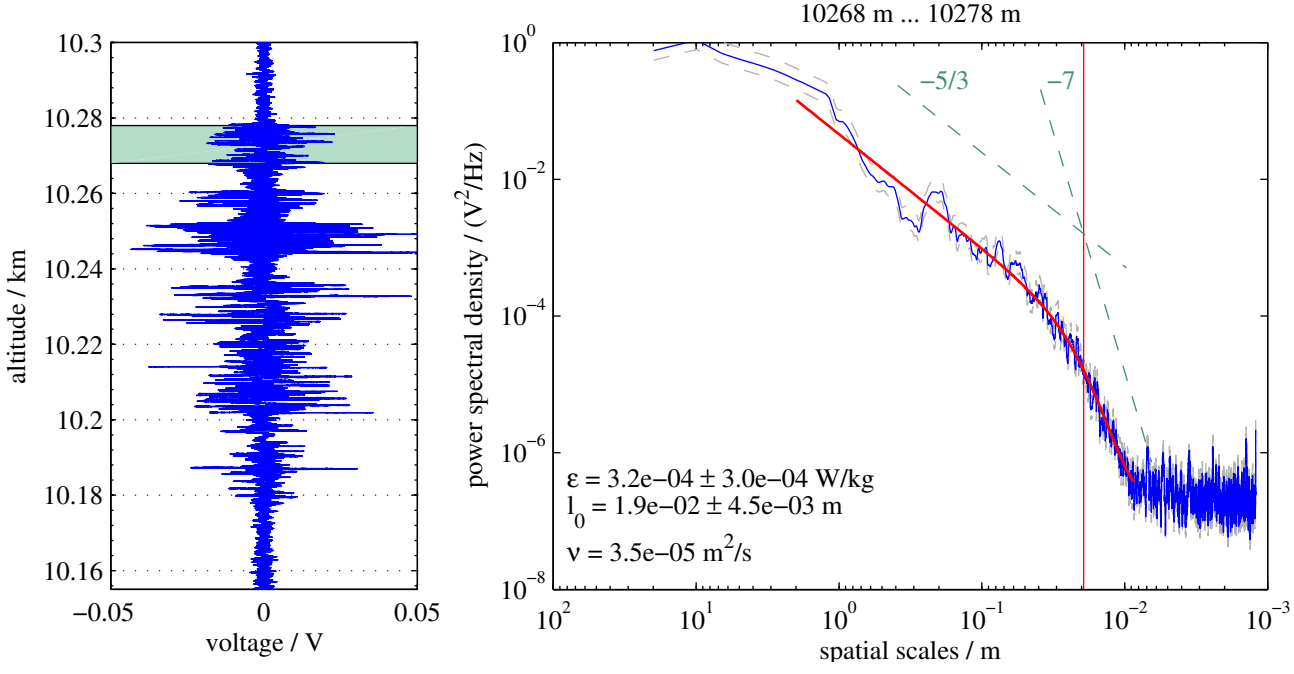

Figure 1. Example of raw data (left) and associated power spectrum (right) computed for the shaded area in the raw data plot. In the raw data, an amplitude of $\lesssim 1$ mV corresponds to instrumental noise. In the spectrum, the blue curve shows the measurement, the grey dashed lines the 95 % confidence interval and the red curve the fit of the Heisenberg model to the measured spectrum, the red vertical line indicates the inner scale l_0. The green dashed lines visualise slopes of $-5/3$ and -7. The errors given are fit errors.

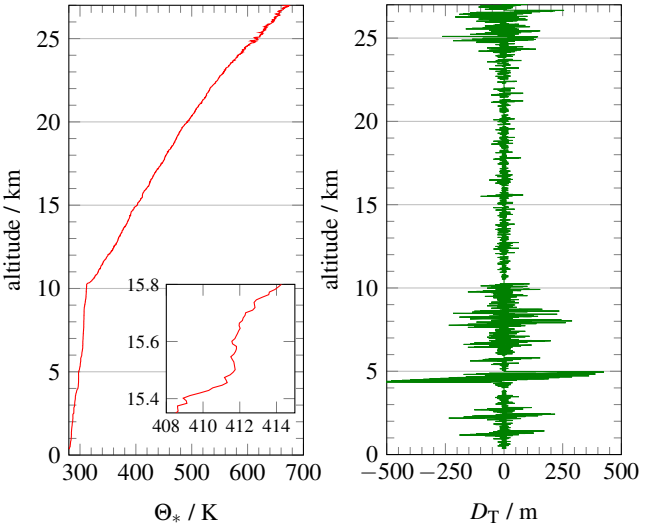

Figure 2. Potential temperature profile (left) and Thorpe displacement (right) for the BEXUS 12 flight. The inset in the left panel shows a magnification from 15.35 to 15.80 km for better visibility of instabilities (manifested as negative gradients of potential temperature).

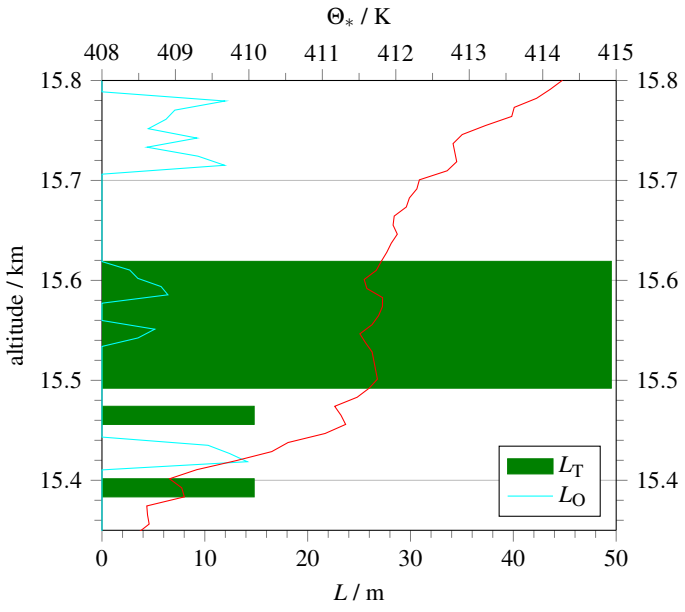

Figure 4. Detail plot of Thorpe (green) and Ozmidov (cyan) scales for the BEXUS 12 flight. The potential temperature is plotted in red.

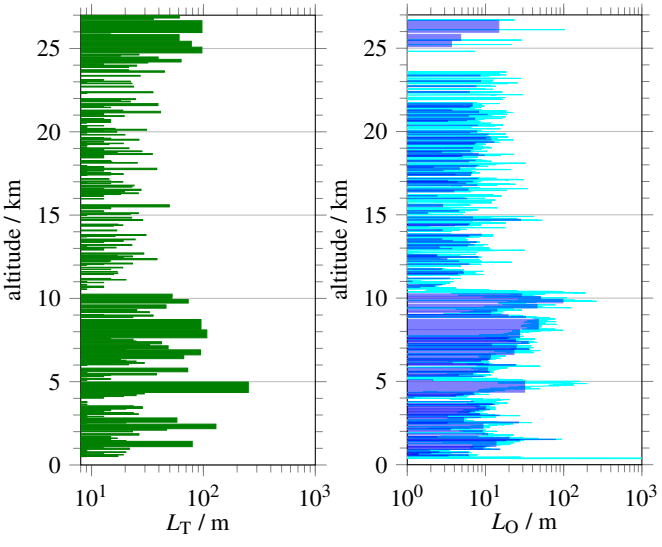

Figure 3. Thorpe length (left) and Ozmidov scale (right) vs. altitude for the detected inversions of the BEXUS 12 flight. The cyan curve shows the Ozmidov scale L_O in the full resolution of the LITOS profile, the blue one averages over the inversions detected by the radiosonde ($\overline{L_O}$).

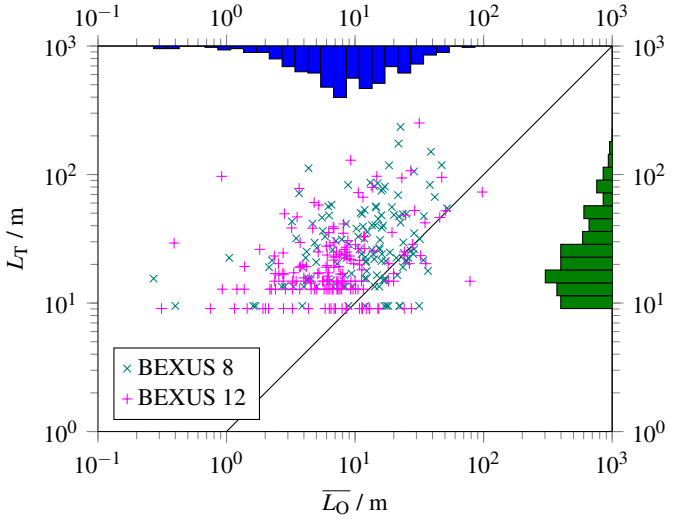

Figure 5. Thorpe scale L_T vs. Ozmidov scale $\overline{L_O}$ for the BEXUS 8 (green) and 12 (magenta) flights. The black diagonal line represents $L_O = L_T$. The histograms show the distributions of L_O and L_T, respectively, of the composite data set of BEXUS 8 and BEXUS 12, i. e. of all data points in the graph. The occurrence axes have a linear scale and are omitted due to readability. Note that L_T is limited by the resolution of the radiosonde ($\sim$ 10 m).

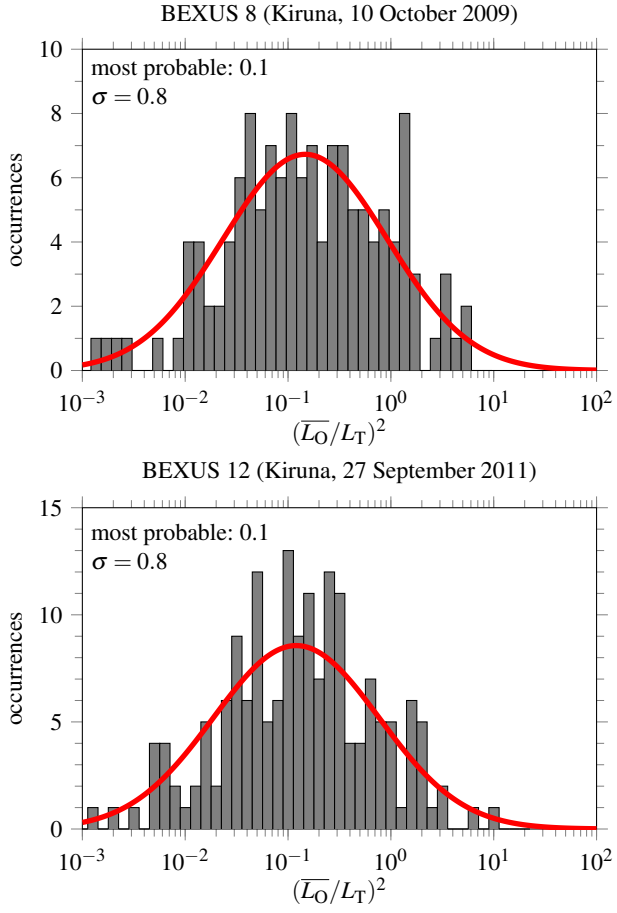

Figure 6. Statistics for the ratio $(\overline{L_O}/L_T)^2$ for the BEXUS 8 (top) and BEXUS 12 (bottom) flights. The red curves show the most likely normal distributions for the logarithmic data.

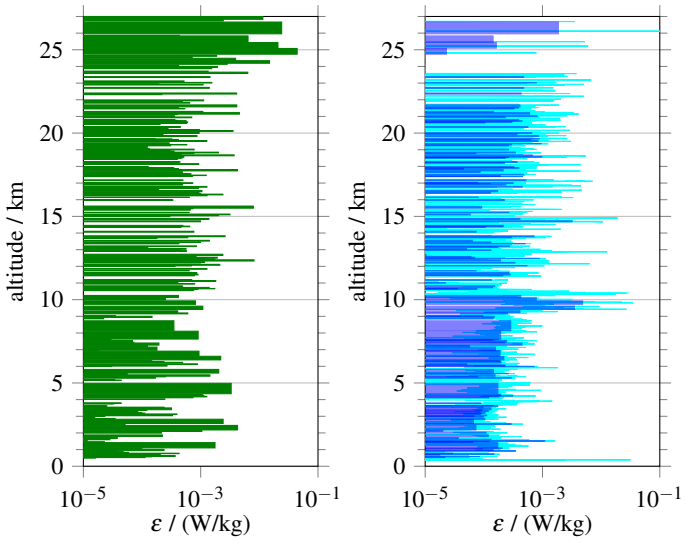

Figure 7. Energy dissipation rates from Thorpe analysis of the radiosonde (left) and spectral analysis of the high-resolved wind measurement (right) for the BEXUS 12 flight. The cyan curve shows ε in the full resolution, the blue one averages over the unstable layers detected by the Thorpe analysis ($\langle\varepsilon\rangle$).

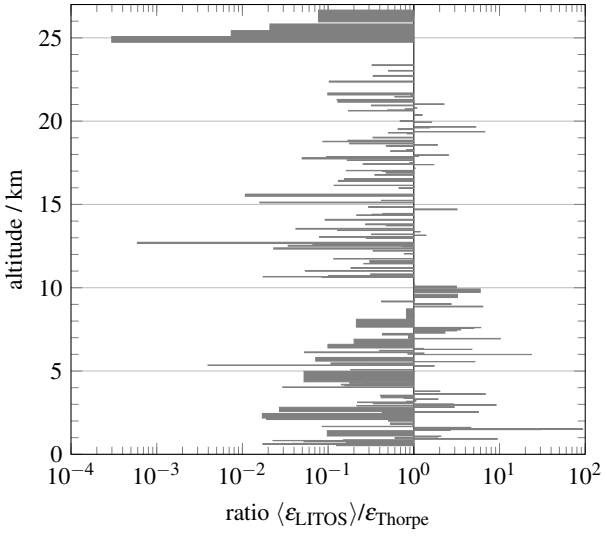

Figure 8. Ratio between energy dissipation rates from spectral analysis and from Thorpe analysis for the significant unstable layers of the BEXUS 12 flight.